Biochimica et Biophysica Acta, 985 (1989) 101–105
Elsevier

BBAMEM 70624

BBA Report

Cross-sectional view of myelin figures

I. Sakurai [1], T. Suzuki [2] and S. Sakurai [2]

[1] *Biophys. Lab., The institute of Physical and Chemical Research, Hirosawa, Wako, Saitama and* [2] *Appl. & Res. Center, Electron Optics Division, JEOL, Akishima, Tokyo (Japan)*

(Received 17 April 1989)

Key words: Myelin figure; Growth mechanism; Phosphatidylcholine; Cryo-stage system; Scanning electron microscopy

Cross-sections of myelin figures from an egg-yolk phosphatidylcholine/water system were observed directly by use of a scanning electron microscope (SEM) equipped with a cryo-stage system, for the first time. Observations were made at a temperature of about −140 °C and at a relatively low magnification so as to obtain an accurate view of the entire structures of myelin figures, as well as the growth behavior of them. The observed internal structures of myelin figures were partly consistent with those in previous reports based upon optical experiments.

Myelin figures are peculiar structures which are found in systems of an amphiphilic molecules and water. From previous observations (e.g., optical and X-ray studies), each of them is thought to be of a multi-lamellar rod like structure in which stacked bilayers of amphiphiles, alternating with water layers, are concentrically wrapped around a rod-like core-axis of water. But the internal structures of myelin figures have not previously been directly observed. The growth behavior and structure of myelin figures have been generally observed only under an optical microscope and accordinly only the external appearance of the figures has been reported on [1,2] (Fig. 1).

Although there have been some previous reports on the observation of sectional views by utilizing replicas taken from the frozen structures of the assemblage of lipid molecules, those reports have focused on the vesicles and particles of phospholipid dispersed in water, and have revealed partly rolled and aggregated structures which have diameters less than 2 μm [3,4]. The inner structures and growth mechanism of the myelin figures, obtained through their cross-sections, have not previously been examined.

By use of a scanning electron microscope (JSM-840A) which was equipped with a cryo-system, the cross-sections of the growing myelin figures were observed at a temperature of about −140 °C. Fig. 2 illustrates the experimental arrangement used to observe the cross-sections of myelin figures. Egg-yolk phosphatidylcholine was put into the hole of a cell made of a cylindrical aluminium block and a drop of pure water was then placed upon the phosphatidylcholine. Immediately, myelin figures started to grow at the phosphatidylcholine/water interface, growing in bunches towards the free water. After about 5 min of growth, myelin figures of between 10 and 20 μm in thickness and several hundred micrometers in length had formed at the phosphatidylcholine/water interface. The cell was then placed into liquid N_2 of −210 °C (a nitrogen slush preparation) for about 5 min. After setting the specimen into the cryo-system of the microscope, the frozen myelin/water system was cut with a knife, which had been already set into the microscope, to observe the cross-section of the specimen.

A specimen of biological cell can suffer from the freezing damage and/or alteration. However, it is reported that such damage and/or alteration of the cell can be avoided or limited by replacing water in and around the cell with a glycerol/water mixture [5,6]. Moor reported that, in the case of yeast cells, specimens frozen in a 20 vol.% glycerol/water solution, in contrast to those treated in water alone, were protected from damage due to freezing regardless of the cooling rate [5]. Accordingly, as a control, we grew myelin figures in a 20 vol.% glycerol/water mixture and observed the cross-sections of myelin figures under the same conditions as we observed the cross-sections of figures grown only in water. By comparing cross-sections taken from figures grown in a 20 vol.% glycerol/water mixture with figures grown only in water, we found that there was little difference between the two samples, at least before etching treatment, and concluded that the freezing

Correspondence: I. Sakurai, Institute of Physical and Chemical Research, Hirosawa, Wako, Saitama 351-01, Japan.

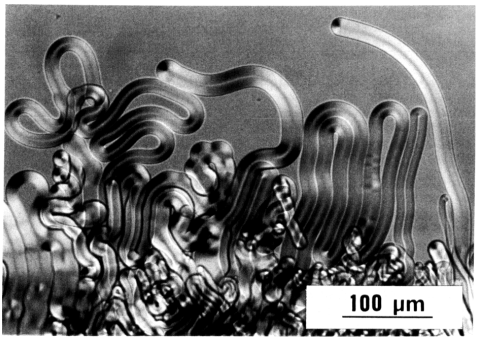

Fig. 1. Myelin figures of phosphatidylcholine/water system observed by a polarizing microscope after about 5 min from the start of growth. These figures have grown in the 50 μm gap between a slide and a cover glasses placed horizontally.

damages did not affect the observed structures of figures grown in water, at least in the observation at low magnification as in the present case.

Fig. 3 is a photograph of the 'as cut' cross-sectional view of myelin figures immediately after an incision was made along cutting plane C1 in Fig. 2, which was taken by use of SEM at about $-140\,^{\circ}C$. This photograph depicts the 'root' region of the myelin figures and, while only loose contours of the figures can be observed, we can see the figures are closely packed and in contact with one another. In order to obtain the more detailed image of the cross-section, the water molecules, which existed in the water cores as well as in the water layers between the stacked bilayers and in the gaps between neighboring myelin figures, were partly evaporated by 'etching' at $80\,^{\circ}C$ for 3 min.

Fig. 4 represents the same portion of the cross-section as appears in Fig. 3 after the etching process, and we are able to see the internal structure of the myelin figures in much greater detail. Each myelin figure con-

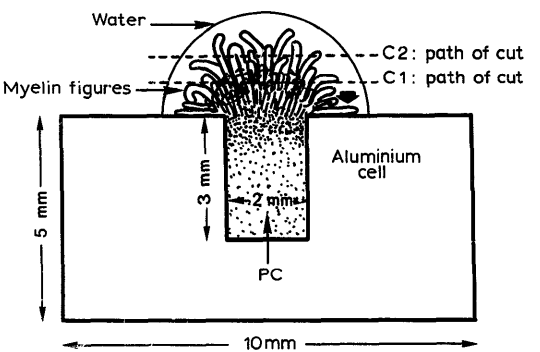

Fig. 2. A schematic representation of the cross-sectional view of observation cell and specimen for SEM observation. PC, phosphatidylcholine.

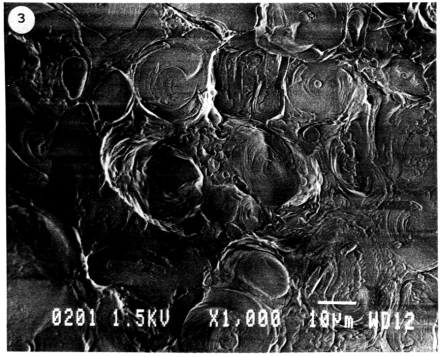

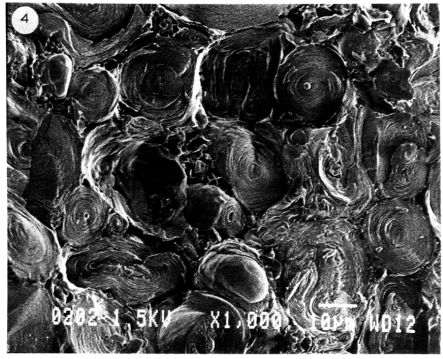

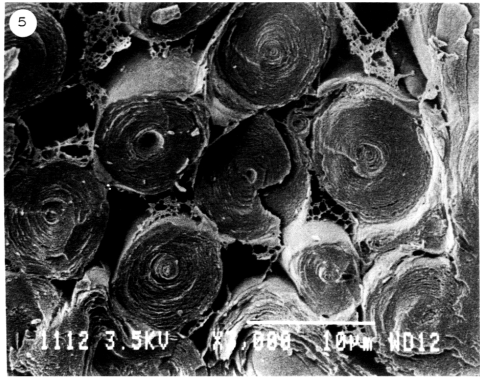

Fig. 3. A cross-sectional view of the myelin figures along C1 in Fig. 2, just after cutting, but prior to the etching process. Accelerating voltage of 1.5 kV, and magnification of ×1000 were used. The white bar in the photograph represents 10 μm.

Fig. 4. The same area as in Fig. 3, but after the etching process. By the etching some amount of water molecules were evaporated. The photograph was taken under the same conditions as for that in Fig. 3. The internal structures of myelin figures can be observed in a greater detail and with a greater contrast. The white bar represents 10 μm.

Fig. 5. A cross sectional view of the tip region of growing myelin figures obtained by cutting along C2 (see Fig. 2). Accelerating voltage of 3.5 kV and a magnification of ×3000 were used. The surface of specimen was treated by a vacuum deposition of gold following etching. The net-like structures between the figures may be residual contaminants including lipids remained after the etching process and/or fragments of stacked bilayers. The white bar represents 10 μm.

sists of a cylindrical roll of stacked bilayers which exist from the outer surface of myelin figures to the figure's center core where water molecules had previously existed. After the etching, we could observe that the stacked bilayers in the cylindrical roll were partially aggregated giving the stripes in the figure. Judging from the magnification of SEM observation, each stripe is an aggregation of several stacked bilayers, although it seems to show the thickness of one layer in stacked bilayers. This aggregation of stacked bilayers occurred during the cooling and etching processes, accompanying probably partial crystallization. A number of chinks were observed in the region of the stacked bilayers. This metamorphosis in the stacked bilayers was due to an anisotropy in the expansion coefficient in the bilayer plane [7,8] which occurs during the course of rapid cooling and etching. The parts of the stacked bilayers along the outer surfaces of those figures were loosely wrapped around the figures' exteriors and were making contact and fusing with neighboring figures. In ad-

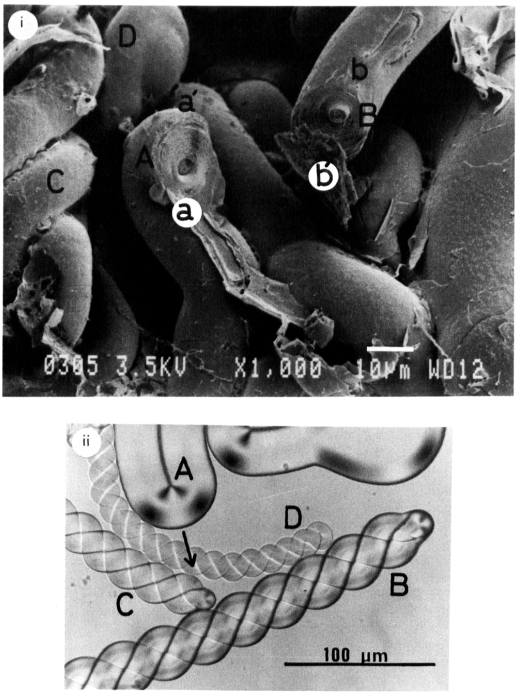

Fig. 6. (i) The outer surface of myelin figures, observed in the direction of the thick arrow in Fig. 2. Cross sections 'A' and 'B' are sections of the same myelin figure cut apart. They are sections of a folded part of myelin figure. The surface of specimen was treated by a vacuum deposition of gold after etching. The tip of a helical form in an early stage of deformation can be seen in (i) D. The white bar represents 10 μm. (ii) Complicated structures of myelin figures under a polarizing microscope. The 'double helix' of myelin figure consists of two simple myelin rods having the same diameter (B, C, and D, and also (i) C). The arrow represents the direction of growth in a folded myelin figure.

dition, we observed fragments of stacked bilayers which seemed not to belong to myelin figures. In contrast, observations of cross-sections taken from figures at cutting plane C2 in Fig. 2, the 'tip' region, revealed that the stacked bilayers along the outer surfaces of the myelin figures were tightly wrapped around the figures' exteriors and generally the figures were only in contact with one another. Furthermore, as Fig. 5 illustrates, fragmented bilayers were not found in the figures tip regions.

Because of their low modulus of bending [9] the myelin figures often bent or 'folded over' while growing. As has been previously reported, the initial growth of myelin figures is diffusion-limited, and the diffusion is along the long axis of myelin figure [1] from the root to the top.

An optical microscope observation revealed that when a figure bent and folded, the outer region at the top of the folded part of the figure became an additional growth point (e.g., Fig. 6(ii) A, the thick arrow shows the additional growth direction). By a cross-section from the folded part in a myelin figure (Fig. 6(i) A and B where B was cut apart from A), we were able to obtain information on the growth mechanism in that region.

As photographs Fig. 6(i) A and B reveal, the water cores of myelin figures are slightly off-centered and biased towards **a** and **b**. Accordingly, the radii from the core of figures are shorter for the core to point **a** or **b** than for the core to point **a'** or **b'**, but the numbers of stacked bilayers which exist along the longer and shorter radii of figures are thought being equal. This equality implies that stacked layers (each layer consists from a lipid bilayer and a water layer) existing along the shorter radius of the figures (core to point **a** or **b**) are thinner than those existing along the longer radius of figures (core to point **a'** or **b'**). Consequently, the difference in the ratio of the thickness between the water layer and the bilayer within each stacked layer should exist between in shorter radius and in longer one. In the longer radius, the ratio of the water layer of the stacked layer is greater than in the shorter one. According to Small [10] the situation implies that the thickness of lipid bilayers in longer radius is less than that of the shorter radius and the surface area occupied by a lipid molecule is smaller in the shorter radius than that in the longer radius. Accordingly, the concentration of lipid molecules in each stacked bilayer is higher in the region of shorter radius than in the longer radius and there exists a concentration gradient of lipid molecules around each stacked bilayer in the cross-sectional plane. In the cross-sectional plane of this folded region, which is perpendicular to the long axis of figure, lipid molecules tends to move in each stacked bilayer from the region of shorter radius towards the that of longer one. The concentration gradient of lipid molecules also exists in the bilayers along the long axis of the myelin figure, higher in the root region and lower in the top region, and lipid molecules tend to move towards the top of the myelin figure from the root region [11]. In addition, a concentration gradient due to a curvature strain in the folded region may also exist along the long axis of myelin figure. These concentration gradients, especially that in the cross-sectional plane perpendicular to the long axis of myelin figure, should drive the growth at the additional growth point at the tip of the folded part as shown in Fig. 6(ii) by an arrow.

In addition, Fig. 6 demonstrates another important feature on the growth mechanism of myelin figure. Fig. 6(i) C represents a helical structure (i.e., a double helix of two simple myelin rods having equal diameters; see Fig. 6(ii) B, C, and D). The outer surfaces of the two myelin rods of a helix are not in close contact except in the top region (Fig. 6(i) D). Optical microscopic observation did not allow us to state conclusively how growth occurs at the tip of the helix structure. However, we can estimate that the helical growth occurs due to a deformation of the loop at the tip of the structure where the two rods of the helix are connected one another, and a new pitch of the helical structure is formed at the tip. Fig. 6(i) D is an example of deformation which occurs at the tip of the twisted helical rods in an early stage of helical growth.

We think that the method described here is useful to clarify the internal structure of complicated myelin figures, which may afford us an opportunity to understand the mechanism of self-organization and self-assembly of the lipid molecules into cell membranes.

The authors are grateful to Dr. H. Sakairi and Dr. Y. Kawamura of The Institute Physical and Chemical Research for his kindness in giving us the opportunity to use SEM and for valuable discussions, respectively.

References

1 Sakurai, I. and Kawamura, Y. (1984) Biochim. Biophys. Acta 777, 347–351.
2 Sakurai, I., Kawamura, Y., Sakurai, T., Ikegami, A. and Seto, T. (1985) Mol. Cryst. Liq. Cryst. 130, 203–222.
3 Kleman, M., Williams, C.E., Costello, M.J. and G.-Krzywicki, T. (1977) Phil. Mag. 35, 33–56.
4 Williams, R.M. and Chapman, D. (1976) Prog. Chem. Fats Other Lipids 15, 33–66.
5 Moor, H. (1973) in Freeze-Etching, Techniques and Applications (Benedetti, E.L. and Favord, P.E., eds.), pp. 11–19, Societe Française de Microscopie Electronique, Paris.
6 Fujikawa, S. (1988) Electron Microsc. Rev. 1, 113–140.
7 Sakurai, I., Sakurai, S., Sakurai, T., Seto, T., Ikegami, A. and Iwayanagi, S. (1980) Chem. Phys. Lipids 26, 41–48.
8 Sakurai, I., Sakurai, T., Seto, T. and Iwayanagi, S. (1983) Chem. Phys. Lipid 32, 1–11.
9 Sakurai, I. and Kawamura, Y. (1983) Biochim. Biophys. Acta 735, 189–192.
10 Small, D.M. (1967) J. Lipid Res., 8, 551–557.
11 Sakurai, I. (1985) Biochim. Biophys. Acta 815, 149–152.